云　南　植　物　研　究　2010，**32**(4)：285～295
**Acta Botanica Yunnanica**　DOI：10.3724/SP.J.1143.2010.10065

# 毛竹茎秆纤维细胞发育过程中的细胞程序性死亡*

甘小洪$^1$，丁雨龙$^2$

（1 西华师范大学西南野生动植物资源保护教育部重点实验室，四川 南充　637009；
2 南京林业大学竹类研究所，江苏 南京　210037）

**摘要**：利用TUNEL检测、细胞学及细胞化学方法，对毛竹茎秆纤维细胞发育过程中的细胞程序性死亡进行了研究。在次生壁形成的早期，纤维细胞出现染色质凝聚、细胞器膨胀、液泡膜解体和细胞质泡状化等典型的细胞程序性死亡形态学特征；TUNEL检测反应呈阳性，显示此时的纤维细胞核DNA发生了片段化。此时，在纤维细胞裂解的液泡膜、降解的细胞质和凝聚的染色质上具有ATPase活性。纤维细胞质的$Ca^{2+}$水平会随着次生壁的形成而逐渐升高，随后$Ca^{2+}$聚集成块状。在初生壁形成后期，纤维细胞染色质上的酸性磷酸酶（APase）活性增强。随着纤维次生壁的持续增厚，ATPase、酸性磷酸酶和$Ca^{2+}$将在裂解的细胞质和凝聚的染色质上持续存在多年。结果表明，毛竹茎秆纤维细胞的次生壁形成过程是一个主动自溶的细胞程序性死亡过程。初生壁形成后期染色质上酸性磷酸酶活性增强及次生壁形成期胞质$Ca^{2+}$的聚集，与纤维细胞的程序性死亡密切相关。ATPase，$Ca^{2+}$和APase参与了纤维细胞程序性死亡过程中原生质体的降解。

**关键词**：纤维细胞；毛竹；细胞程序性死亡；超微结构；超微细胞化学

**中图分类号**：Q 944，Q 945　　**文献标识码**：A　　**文章编号**：0253-2700(2010)04-285-11

# Programmed Cell Death during Fiber Cell Development in *Phyllostachys edulis*（Poaceae）Culm

GAN Xiao-Hong$^1$，DING Yu-Long$^2$

（1 *Key Laboratory of Southwest China Wildlife Resources Conservation (Ministry of Education)*，
*China West Normal University*，Nanchong 637009，China；2 *Bamboo Research Institute*，
*Nanjing Forestry University*，Nanjing 210037，China）

**Abstract**：Programmed cell death during fiber cell development in *Phyllostachys edulis* culms was studied by using the TUNEL assay，and the cytological and cytochemical methods. At the early stage of secondary wall formation，the morphological features of PCD such as chromatin agglutination，organelle swelling，and the tonoplast disintegration and cytoplasm vacuolation were investigated in fiber cells. Positive signals by TUNEL assay could be also detected which evidenced the nDNA fragmentation. $Mg^{2+}$-ATPase activity was examined on the cleavage tonoplast，disintegrated cytoplasm and agglutinated chromatin of fiber cells at that time. The level of $Ca^{2+}$ in fiber cytoplasm would increase with secondary wall formation，and $Ca^{2+}$ would be congregated densely. APase was sparsely localized on the nuclear chromatin during primary wall formation，but it was densely aggregated at the late stage. With the continual thickening of secondary wall，the cleavage cytoplasm and agglutinated chromatin with the activity of $Mg^{2+}$-ATPase and APase in fiber cells were persistent for many years，and $Ca^{2+}$ was also detected in these structures. The results showed that secondary wall formation of fiber in *P. edulis* culm was an active autophagic PCD，and the aggregation of $Ca^{2+}$ in cytoplasm during secondary wall formation and APase densely localized on the nuclear chromatin during late primary

---

* Foundation items：The Startup Fund for Scientific Research of China West Normal University（No. 05B035）and the National Natural Science Fund of China（No. 30271064）

Received date：2010-03-25，Accepted date：2010-06-17

作者简介：甘小洪（1974－）男，汉族，副教授，主要从事发育植物学、植物资源保护与利用研究。

wall formation, were correlated to the occurrence of fiber PCD. $Mg^{2+}$-ATPase, $Ca^{2+}$ and APase were all involved in the disintegration of fiber protoplast during PCD.

**Key words**: Fiber cell; *Phyllostachys edulis*; Programmed cell death; Ultrastructure; Ultracytochemistry

Bamboos are economically important plants with innumerous uses such as making furniture, construction, pulp and paper, and other industries. As one of important components of bamboo culms, the structure and properties of fiber have a decisive impact on the property of bamboo culms, and in turn, dramatically influence culm utilization (Gan and Ding, 2005). Several investigations have dealt with the morphology, chemical components and tissue ratio of fibers, which correlate to the strength of the culm and its pulping properties (Shigematsu, 1940; Ghosh and Negi, 1959; Liese and Grosser, 1972; Espiloy, 1987; Abd. Latif, 1995), and the fine structure of bamboo fibers had also been investigated in detail (Tono and Ono, 1962; Parameswaran and Liese, 1976, 1980; Fujii, 1985). The successive development of bamboo fiber cells could be divided into three stages: formation of fiber initials, primary wall and secondary wall. The multilamellate structure and thickening of fiber cell wall were observed with the development of a culm and further ageing (Murphy and Alvin, 1992; Liese and Weiner, 1996; Gan and Ding, 2005). The plasmolysis and apoptotic bodies investigated during early secondary wall formation of fiber cell in *Phyllostachys edulis* culm, revealed the occurrence of programmed cell death (PCD) (He *et al.*, 2000).

PCD is considered as an integral part of development in plants. Such an inbuilt death programme is triggered in response to internal or external signals, and plays an important role in plant normal development, such as terminal differentiation of tracheary elements and lysigenous aerenchyma formation (McCann *et al.*, 2000; van Doorn and Woltering, 2005; Gunawardena, 2008), senescence of peripheral rootcap cells (Zhu and Rost, 2000) and leaves (Cao *et al.*, 2003; Gunawardena *et al.*, 2007). PCD is often associated with the occurrence of specific biochemical and morphological features such as condensation of the nucleus and cytoplasm, fragmentation of nuclear DNA (nDNA) (Cao *et al.*, 2003; Gunawardena *et al.*, 2005). Wherein, nDNA fragmentation is the hallmark of PCD, which can be detected by the TUNEL assay (Groover *et al.*, 1997). No is known about the changes of nDNA during fiber cell secondary wall formation or fiber PCD so far.

In plants, as in animals, PCD is an energy dependent process. Plant cell undergoing PCD is an active participant in its own demise ("cellular suicide"). ATP is an essential energy currency in nature and its role in cellular metabolism is well established, and ATPase plays a key role in the energy release during these processes (Cui, 1997). By using the cytochemical localization of ATPase, the cell components actively participating in plant cell metabolism and ontogeny could be detected (Wang *et al.*, 2000). Nothing is known about the dynamic changes of ATPase activity during development of bamboo fibers.

APase (Acid phosphatase) is a non-specific hydrolytic enzymes essential to phosphate esters, carbohydrate and phosphate metabolism, and important for phosphorus scavenging and remobilization in plants (Darleen *et al.*, 1989; Cashikar *et al.*, 1997). Massive evidences demonstrate that APase has crucial roles in metabolism of cell wall, intercellular nutrient transportation and phosphate transfer reaction (Tian and Shen, 1994; Wang *et al.*, 1999; Ibrahim *et al.*, 2002; Ferten *et al.*, 2003). During secondary xylem differentiation, APase was reported to play functions in PCD by Wang *et al.* (1999).

As an important second messenger in plants, calcium played important roles during the growth and development of plant, such as cell division, cell wall formation and polarity growth, as well as PCD (White and Broadley, 2003). During the differentiation of tracheary elements, $Ca^{2+}$ participated in the PCD and thickening of cell wall (Groover and Jones, 1999). Little is known about the functions of $Ca^{2+}$ on fiber PCD.

The aim of the study was to improve the understanding of fiber PCD in bamboo culms. Three specific questions were answered by using different methodology such as TUNEL (terminal deoxynucleotidyl transferased UTP nick end labeling) assay, cytological and cytochemical methods: (1) Did fiber PCD occur accompanying with secondary wall formation of fiber cell? (2) What was the reason resulting in fiber PCD during secondary wall formation? (3) What roles did ATPase, $Ca^{2+}$ and APase played in fiber PCD?

## Materials and Methods

### Plant material

Young shoots and culms of 1 to 8-year-old *Phyllostachys edulis* Mazel ex H. de Leh. were harvested in May 2003 at the Bamboo Garden of Nanjing Forestry University. Young shoots with the heights of 60 cm, 80 cm, 120 cm and 700 cm were collected, and all samples from the middle part of the culm wall were taken as the method by Gan and Ding (2005).

### Light microscopy and TUNEL assay

The blocks were fixed in 2% glutaraldehyde in 0.02 millimole (mM) sodium cacodylate buffer (pH 7.0) for 4 h at room temperature, dehydrated in a graded ethanol series, and embedded in Technovit 7100 resin. Continued sample sections (5 μm in thickness) mounted on glass slides were first examined and photographed under an Olympus BH-2 polarizing microscope, then treated with the *in situ* Cell Death Detection Kit AP according to the manufacturer's instructions (Roche, Germany). For positive control, DNase Ⅰ (grade Ⅰ, 0.5 mg·$ml^{-1}$ in 50 mM Tris-HCl, pH 7.5, 1 mg·$ml^{-1}$ BSA) was added before TUNEL reaction mixture for 10 min at room temperature to induce DNA strand breaks. The negative control was conducted by similar incubations in the absence of TdT. Samples were counter-stained with 0.5% methyl green for 30 s.

### Transmission electron microscopy

Samples were prefixed for 2 hours in 0.025 mol·$L^{-1}$ phosphate buffer solution (pH 7.0) containing 4% (v/v) glutaraldehyde in the case of young shoots and 1-year-old culm, or 6% (v/v) glutaraldehyde in the case of 2 to 8-year-old culms. After washing with the same buffer, the samples were post-fixed in 1% $OsO_4$ (also in the same buffer). Followed by a further washing with the buffer, the specimens were dehydrated in a graded ethanol series and embedded in Epon812 resin. After cutting with a diamond knife on a LKB-V ultramicrotome, ultrathin sections were stained with saturated aqueous uranyl acetate for 5 min, followed by staining with lead citrate for 5 min. All sections were examined and photographed with an H-600 (Hitachi, Tokyo, Japan) transmission electron microscope (TEM).

### Ultracytochemical localization of $Mg^{2+}$-ATPase

Following prefixation in a mixture of 4% paraformaldehyde and 2.5% glutaraldehyde, the samples were treated as the method by Wang *et al.* (2000). The control specimens were dealt without substrate, or with substrate in the presence of 10 mM sodium fluoride (NaF). Made with LKB-V ultramicrotome, ultrathin sections of control material were stained with uranyl acetate, but experimental samples no stained. All sections were observed and photographed using an H-600 TEM.

### Ultracytochemical localization of $Ca^{2+}$

After pre-fixed in a mixture of 2% potassium pyroantimonate and 2.5% glutaraldehyde in 0.1 mM sodium cacodylate buffer (pH 7.1) for 3 h at 4℃, the samples were washed with the same buffer, and then post-fixed in a mixture of 2% potassium pyroantimonate and 1% $OsO_4$ in the same buffer. Followed by a further washing with the redistilled water for 4 times, the specimens were washed with the redistilled water (pH 7.6) for 2 times. Afterwards, all specimens were dehydrated in a graded ethanol series and embedded in Epon812 resin. The ultrathin sections were made with LKB-V ultramicrotome, and stained with uranyl acrtate. All sections were observed and photographed using an H-600 TEM.

The treatment of control samples: after examined with an H-600 TEM, the ultrathin sections congregated with calcium pyroantimonate were treated in 100 mM EGTA (ethylene glycol tetraacetic acid) (pH 8.0) for 0.5 −1 h at 60℃. Then these sections were observed and photographed with an H-600 TEM.

### Ultracytochemical localization of APase

After pre-fixed in a mixture of 4% paraformaldehyde and 2.5% glutaraldehyde in 0.05 mM sodium cacodylate buffer (pH 7.2) for 2 h at 4℃, the samples were washed in the same buffer at 4℃ for 1.5 h, and were dissected into slices of about 0.5 mm in thickness in the buffer, and then rinsed with 0.05 mM Tris-maleate buffer (pH 5.0) for 1.5 h prior to enzyme reaction.

The enzyme reaction procedure was performed following the method by Wang *et al.* (1999). The specimens were incubated in a complete reaction medium (50 mM Tris-maleate buffer, pH 5.0, 3.6 mM Pb ($NO_3$)$_2$ and 10 mM sodium β-glycerophosphate) at 37℃ for 2 h. The control specimens were respectively incubated in the same medium but without substrate, or with substrate in the presence of 10 mM sodium fluoride (NaF). After incubation, all specimens were rinsed with 0.05 mM Tris-maleate buffer (pH 5.2) for 1.5 h at 4℃, and then rinsed with 0.05 mM sodium cacodylate (pH 7.2) buffer for 1.5 h at the same temperature. Following this, these samples were fixed at 4℃ with 1% osmium tetroxide in the same buffer overnight. Then all specimens were dehydrated stepwise in an acetone series at 4℃. Specimens were embedded in Epon 812. Ultrathin sections of control specimens were stained with uranyl acetate, while others were not. All sections were viewed and photographed with an H-600 TEM.

## Results

### Light microscopy and TUNEL assay

The fiber cap (vascular strands sheath), vessel elements (protoxylem vessel and metaxylem vessel) and phloem were easily distinguished with the light microscopy (Fig. 1: a). Locations of secondary cell wall are visible under the polarizing microscope: secondary cell wall is strongly anisotropic and shows substantial double refraction and appears bright in polarized light (Esau, 1977). In the middle part of shoot with the height of 60 cm, vessel elements and sieve tube were visible in the vascular strands due to the abrupt increase in wall brightness, while fibers in fiber cap were invisible (Fig. 1: b). At the present time, the fibers were not labeled by TUNEL assay (Fig. 1: c). In the lower part of the same shoot, fiber wall was visible under polarized microscope (Fig. 1: d), and positive signals of TUNEL assay (indicated by purple staining) was detected in the fibers (Fig. 1: e). In negative control sections, no TUNEL-positive reaction were detected in the fiber nuclei (Fig. 1: f).

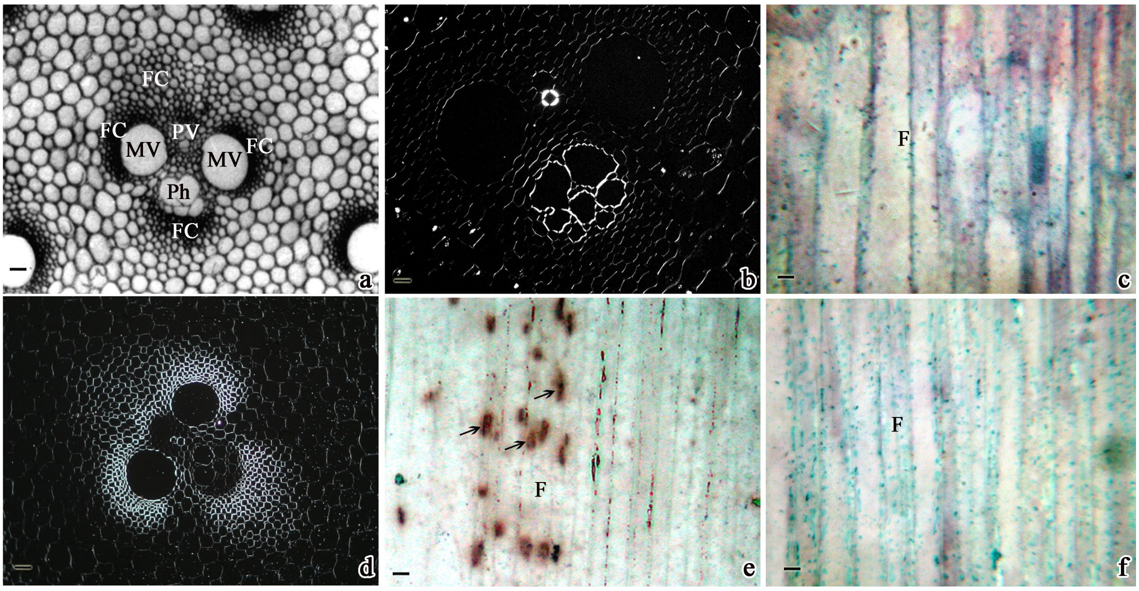

Fig. 1 a: the vascular bundle with lignified fiber cap in *P. edulis* shoot with the height of 700 cm, TS; b-f: the microscopy of shoots with the heights of 60 cm; b: the fibers cell wall were invisible in the middle part of shoot under polarizing microscope which indicated the developmental stage of primary cell wall formation, TS; c: the fibers in the middle part of shoot were not labeled by TUNEL assay, LS; d: the fiber cell wall in the lower part of young shoot was visible due to the abrupt increase in wall brightness, which indicated the developmental stage of secondary cell wall formation, TS; e: TUNEL assay revealed positive signals (purple staining, arrowhead) in the fibers in the lower part of shoot, LS; f: the negative control, showing no TUNEL positive signal in fibers in the lower part of shoot, LS. Bar=10 μm. **Abbreviations**: F: fiber; FC: fiber cap; MV: metaxylem vessel; Ph: phloem; PV: protoxylem vessel; LS: longitudinal section; TS: transverse section

### Transmission electron microscope assay during secondary wall formation of fibers

Early, fiber cell wall thickened billowingly, and intact double karyotheca remained in fiber nucleus, wherein chromatin commenced to agglutination and nucleolus disappeared. However, some organelles such as mitochondrion and rough endoplasmic reticulum and Golgi bodies remained in these cells (Fig. 2: a). With continual thickening of secondary wall, fiber organelles including mitochondrion and rough endoplasmic reticulum gradually swelled and disintegrated (Fig. 2: b). Afterwards, fiber cytoplasm gradually vacuolated, and double karyotheca of nucleus disappeared (Fig. 2: c). Nevertheless, plasma membrane, plasmodesmata and nucleus with the agglutinated chromatin remained in the fiber cells of 6-year-old culms (Fig. 2: f). Along with secondary wall formation, fiber cell wall underwent continual thickening, and polylaminate structures arranged in regular alteration of broad and narrow lamellae appeared (Fig. 2: d-e).

### The dynamic changes of $Mg^+$-ATPase during secondary wall formation of fiber cells

Early, $Mg^+$-ATPase activity was detected on the plasma membrane, tonoplast, nucleus, pits and plasmodesmata and mitochondrion (Fig. 3: a-b). Afterwards, $Mg^+$-ATPase was examined on the annulate lamella and the agglutinated chromatin (Fig. 3: c). With continual thickening of secondary cell wall, the activity of $Mg^+$-ATPase in agglutinated chromatin would increase (Fig. 3: e), and $Mg^+$-ATPase were densely localized on the disintegrated tonoplast (Fig. 3: d) and in the vacuolated cytoplasm (Fig. 3: f). During fiber cell secondary wall formation, $Mg^+$-ATPase remained on the plasma membrane, transfer vesicles in pit channels and plasmodesmata and cytoplasm remnants. The activity of $Mg^+$-ATPase on the agglutinated chromatin

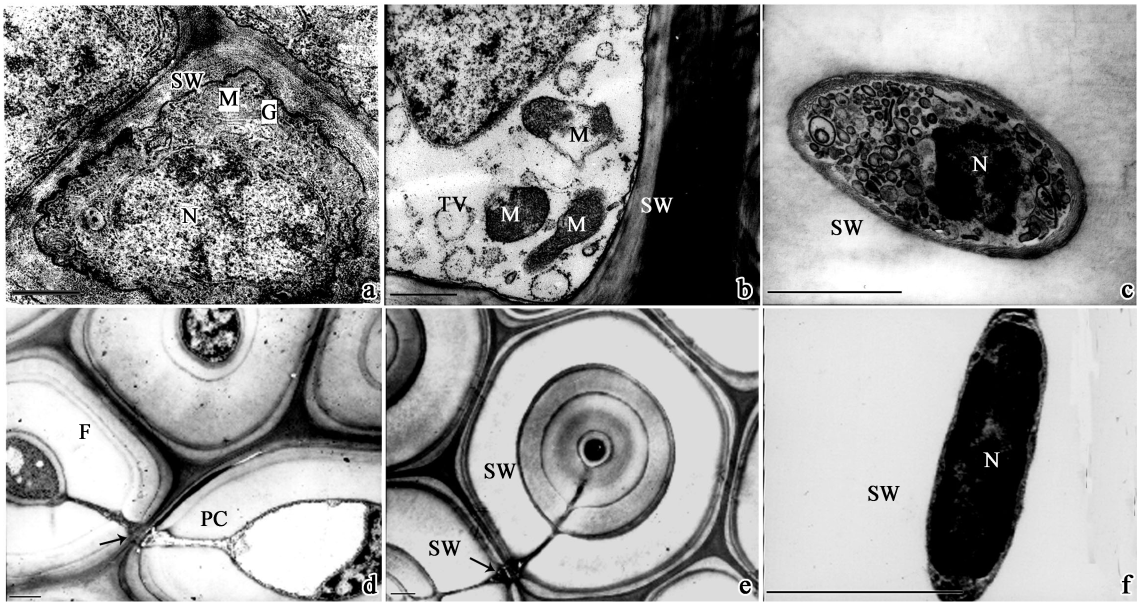

Fig. 2　The ultrastructural modifications of fiber cells during secondary wall formation. a: the fiber cell at the early stage of secondary wall formation, showing billowingly thickening of cell wall, chromatin commenced to agglutination and some organelles remained in the cells, TS; b: ultrastructure of fiber cell in bamboo shoot, showing the agglutinated chromatin, disintegrated mitochondrion and transfer vesicles, TS; c: showing the vacuolated cytoplasm and agglutinated chromatin of a fiber cell in one-year-old culm, TS; d: fiber cells in two-year-old culm, showing the thickening secondary wall of fiber cells and the plasmodesmata (arrow) between fibers, TS; e: the fibers in four-year-old culm, showing polylaminate structures of fiber secondary wall and the plasmodesmata (arrow) between fiber cells, TS; f: showing the agglutinated chromatin of a fiber cell in six-year-old culm, TS. Bar=1 μm. **Abbreviations**: G: Golgi bodies; M: mitochondrion; N: nucleus; PC: parenchyma cell; SW: secondary cell wall; TV: transfer vesicle; TS see Fig. 1

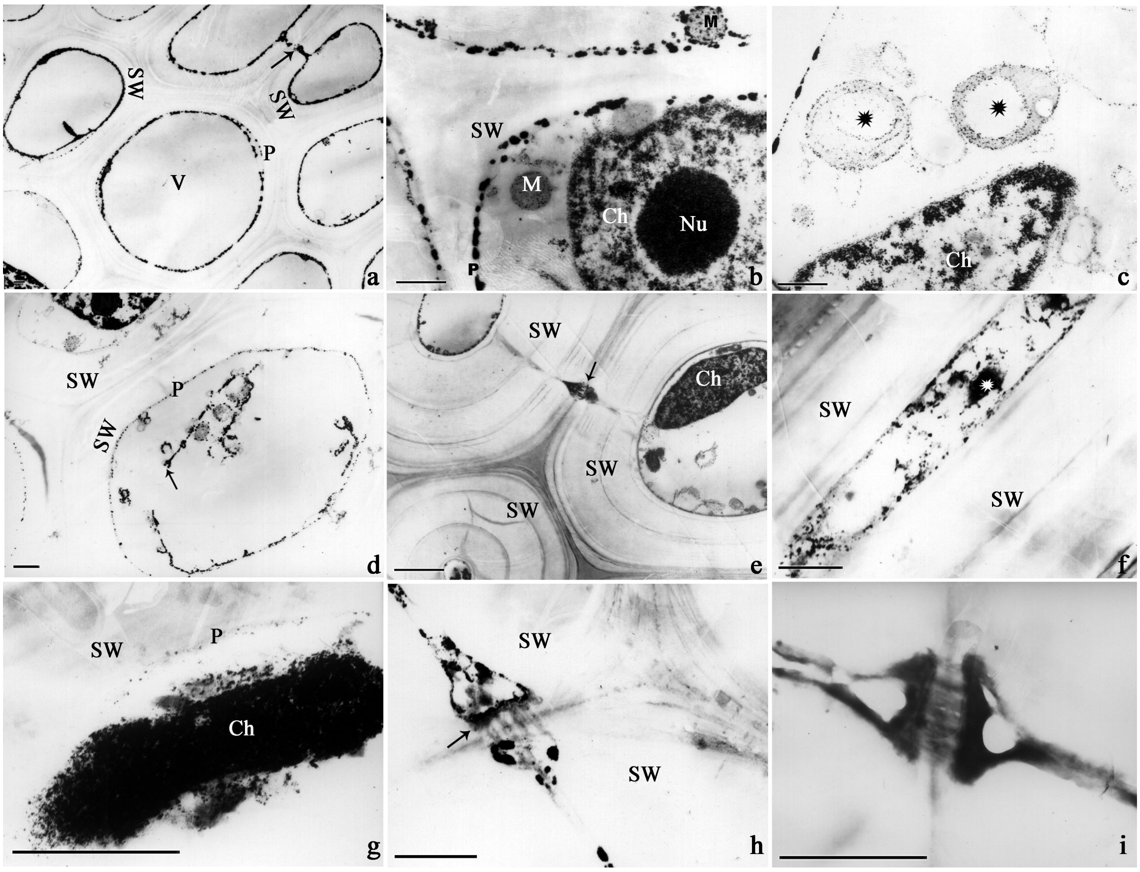

Fig. 3　Dynamic changes of Mg$^{2+}$-ATPase in the fibers during secondary wall formation. a-b: fiber cells at the early stage of secondary wall formation; a: showing the distribution of Mg$^{2+}$-ATPase on the plasma membrane, tonoplast and the plasmodesmata (arrow), TS; b: showing Mg$^{2+}$-ATPase aggregated in mitochondrion and nucleus and on the plasma membrane, TS; c: showing Mg$^{2+}$-ATPase localized on the annulate lamella (star) and agglutinated chromatin in the fiber cells, TS; d: showing dense Mg$^{2+}$-ATPase distributed on the disintegrated tonoplast (arrow) and plasma membrane, TS; e: showing the distribution of Mg$^{2+}$-ATPase on the plasmodesmata (arrow) and agglutinated chromatin of fibers in 1-year-old culm, TS; f: showing the distribution of Mg$^{2+}$-ATPase on the vacuolated cytoplasm (star) of fiber cells in 2-year-old culm, TS; g-h: a fiber cell in 6-year-old culm; g: showing the plasma membrane and agglutinated chromatin with Mg$^{2+}$-ATPase activity, TS; h: showing the plasmodesmata (arrow) with Mg$^{2+}$-ATPase activity between fiber cells, TS; i: showing little Mg$^{2+}$-ATPase detected on the fiber cells in the control specimen with substrate in the presence of 10 mM sodium fluoride (NaF), TS. Bar=1 μm. **Abbreviations**: Ch: chromatin; M: mitochondrion; N: nucleus; Nu: nucleolus; P: plasma membrane; SW: secondary wall; V: vacuole; TS see Fig. 1

would increase with aging (Fig. 3: g-h).

Little Mg$^{+}$-ATPase activity was detected in the control specimens (Fig. 3: i), which demonstrated that the results above were credible.

**The dynamic changes of Ca$^{2+}$ during fiber development**

During fiber initials formation, Ca$^{2+}$ mainly distributed on the cell wall (Fig. 4: a). During early primary wall formation, Ca$^{2+}$ sparsely appeared in the inner side of tonoplast in fiber cells, and some was also examined in phagosome and vacuole (Fig. 4: b). Afterwards, the level of Ca$^{2+}$ in vacuole increase, but little was seen in nucleus and cell wall (Fig. 4: c). At the late stage, massive Ca$^{2+}$ assembled in the cytoplasm, but the level of Ca$^{2+}$ in vacuole decreased, and Ca$^{2+}$ disappeared in cell wall and nucleus (Fig. 4: d). With the formation of secondary wall, the level of Ca$^{2+}$ in fiber cell cytoplasm gradually increased (Fig. 4: e), and then Ca$^{2+}$ densely congregated in fiber cell cytoplasm (Fig. 4: f). During secondary wall formation, Ca$^{2+}$ remained in the disintegrated cytoplasm, agglutinated chromatin, and pit channel and transfer vesicles for many years (Fig. 4: g-h).

The reaction granules of $Ca^{2+}$ disappeared in the fiber cell of the control specimens (Fig. 4: i), which indicated that the results above were credible.

**The dynamic changes of APase during the process of fiber development**

During early primary wall formation, the APase activity was examined on the plasma membrane, tonoplast, karyotheca and nuclear chromatin in fiber cells (Fig. 5: a-b). At the late stage, APase was aggregated on the nuclear chromatin of fiber cells, and some remained on the plasma membrane, tonoplast and vacuolated cytoplasm in fiber cells (Fig. 5: c-d). With the formation of fiber secondary wall, APase was deposited on the plasma membrane, the disintegrated cytoplasm, mitochondrion, and tonoplast and the agglutinated chromatin (Fig. 5: e-f). Along with the continual thickening of secondary wall, APase remained on the plasma membrane, plasmodesmata, plasma membrane invagination and transfer vesicles and agglutinated chromatin

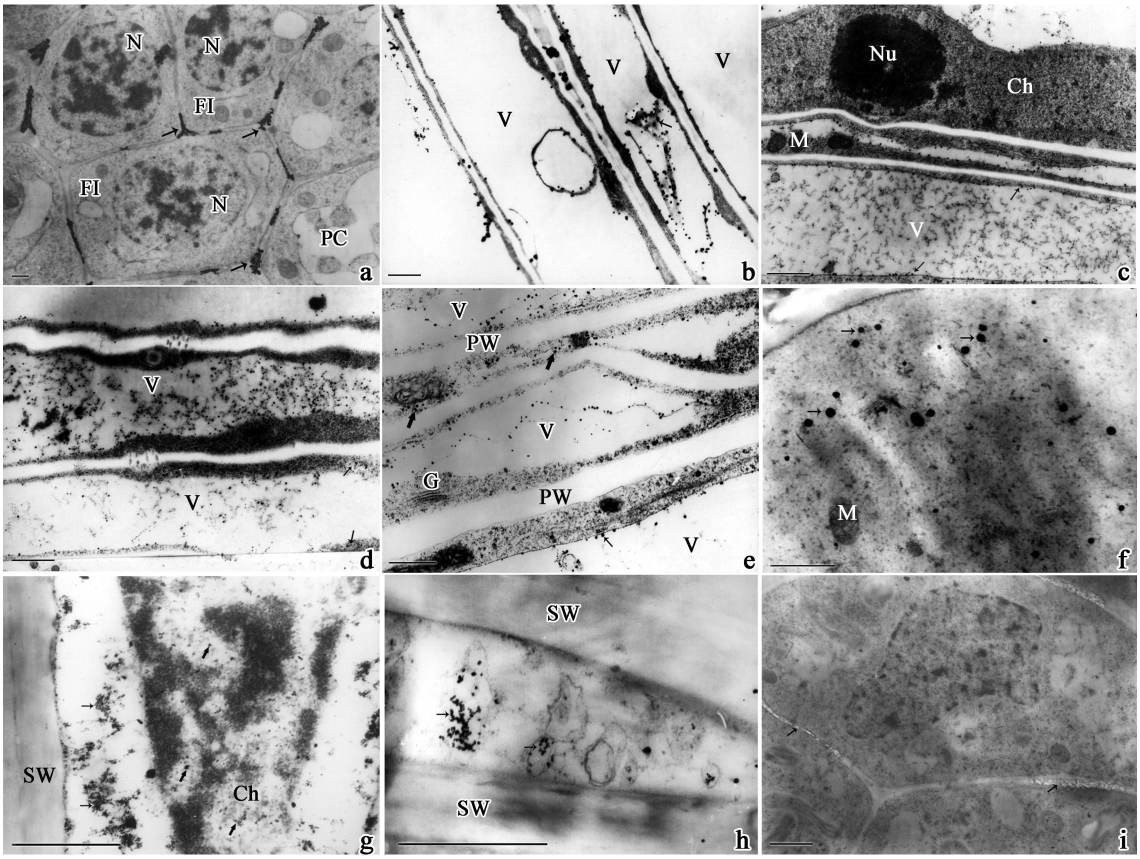

Fig. 4　Dynamic changes of $Ca^{2+}$ in the fiber cells during development. a: fiber initial cells, showing $Ca^{2+}$ localized in the cell wall (arrow), TS; b-e: fiber cells during primary wall formation, LS; b: showing the distribution of $Ca^{2+}$ in the disintegrated cytoplasm (arrow) in vacuole and on the fiber cell wall; c: showing massive $Ca^{2+}$ accumulated in vacuole and some appeared in the inner side of tonoplast (arrow); d: showing the level of $Ca^{2+}$ in vacuole decreased and some assembled in the cytoplasm (arrowhead); e: showing the level of $Ca^{2+}$ in cytoplasm increased (big arrowhead) and some distributed in the inner side of tonoplast (small arrowhead); f: showing $Ca^{2+}$ congregated densely in fiber cell cytoplasm (arrowhead) at the early stage of secondary wall formation, TS; g-h: fiber cells in 4-year-old culm, LS; g: showing $Ca^{2+}$ remained in the disintegrated cytoplasm (small arrowhead) and agglutinated chromatin (big arrowhead) of fiber cells; h: showing $Ca^{2+}$ detected in the vacuolated cytoplasm; i: showing the reaction granule of $Ca^{2+}$ disappeared in the fiber cell of the control specimens, TS. Bar=1 μm. **Abbreviations**: Ch: chromatin; FI: fiber initial cell; M: mitochondrion; N: nucleus; Nu: nucleolus; PC: parenchyma cell; PW: primary wall; SW: secondary wall; V: vacuole; LS, TS see Fig. 1

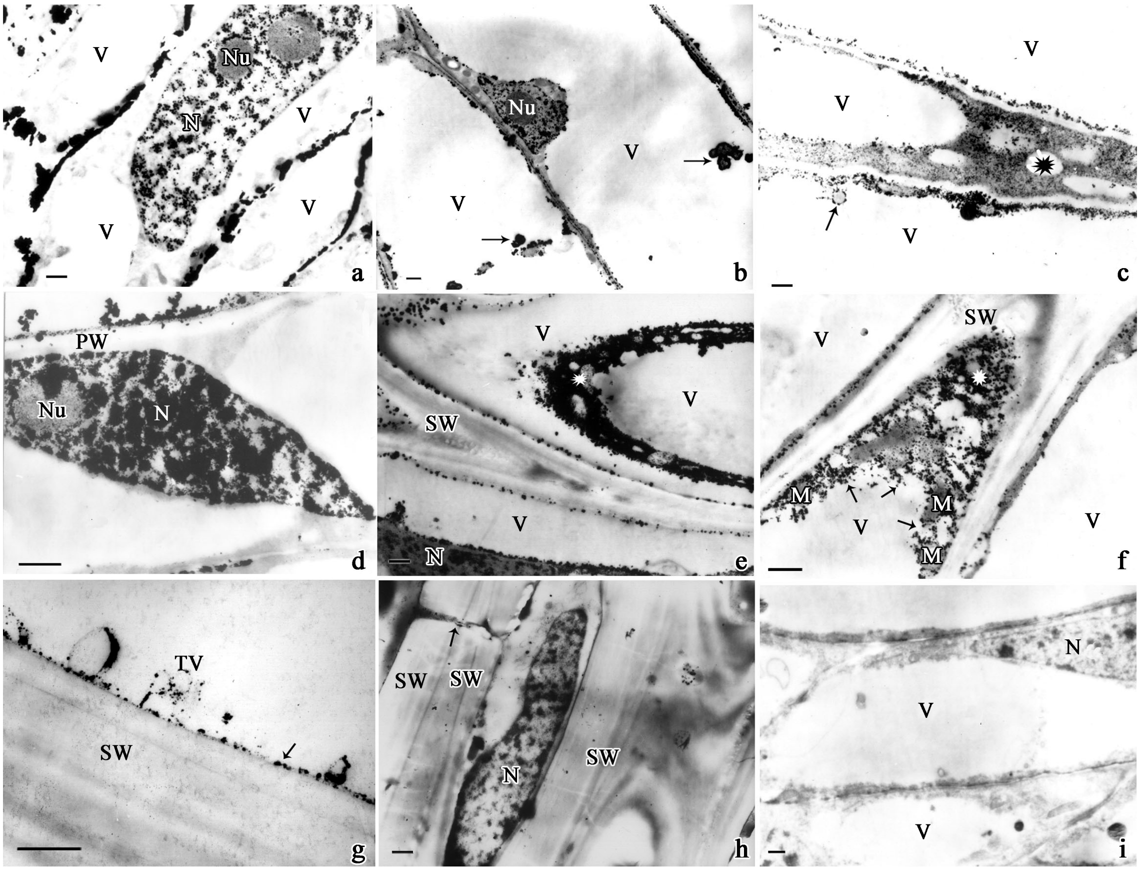

Fig. 5 Dynamic changes of APase during fiber development. a: fiber cells at the early stage of primary wall formation, showing APase distributed on the plasma membrane, tonoplast, karyotheca and nuclear chromatin, LS; b: fiber cells during primary wall formation, showing APase localized on the plasma membrane, tonoplast, chromatin and disintegrated protoplast in vacuole (arrow), LS; c-d, fiber cells at the late stage of primary wall formation; c: showing APase congregated in the vacuolated cytoplasm (star) and transfer vesicle (arrow) in vacuole, LS; d: showing APase detected in the nuclear chromatin; e-f, fiber cells at the early stage of secondary wall formation, LS; e: showing the distribution of APase in the agglutinated chromatin, plasma membrane and the vacuolated cytoplasm (star), LS; f: showing APase distributed on the plasma membrane, vacuolated cytoplasm (star), mitochondrin and disintegrated tonoplast (arrowhead), LS; g: the fibers in 4-year-old culm, showing APase localized on plasma membrane (arrowhead) and transfer vesicle, LS; h: fiber cells in 6-year-old culm, showing APase remained in agglutinated chromatin and plasmodesmata between fibers (arrow), LS; i: showing little APase detected on the fiber cells in the control specimen with substrate in the presence of 10 mM sodium fluoride (NaF), LS. Bar=1 μm. **Abbreviations**: M: mitochondrion; N: nucleus; Nu: nucleolus; PW: primary wall; SW: secondary wall; TV: transfer vesicle; V: vacuole; LS see Fig. 1

of fiber for many years (Fig. 5: g-h).

Little APase was detected in the fiber cell of the control specimens (Fig. 5: i), which indicated that the results above were credible.

## Discussion

At the early stage, the fiber cells in *P. edulis* culms displayed cytological changes such as chromatin agglutination, organelle swelling, tonoplast disintegration and cytoplasm cleavage, which indicated the *in situ* autolysis of fiber cell protoplasts, and the typical morphological features of PCD (Wang *et al.*, 1999; Fukuda, 2000; Andrea *et al.*, 2008). Along with the PCD, the cell wall underwent continual thickening with aging, and the poly-laminate structure of the cell wall in alternate arrangement of narrow and broad lamellae also formed gradually. The ultrastructural changes evidenced that secondary wall formation of fiber cell accompanied with the

PCD. The disintegrated protoplasts due to PCD was not be absorbed by surrounding cells as reported by Jones (2001), but was used to build its cell wall like tracheary elements (Fukuda, 2000; Cui, 2000).

TUNEL assay was performed with the aim of understanding specific degradation of nucleus (Mittler and Lam, 1995). During primary wall formation, fiber cells were not labeled by TUNEL assay, but positive signals (indicated by purple staining) could be detected in the fiber cells during early secondary wall formation, which revealed the DNA degradation accompanying with secondary wall formation.

During secondary wall formation, $Mg^{2+}$-ATPase remained in nuclear chromatin of fiber cells in *P. edulis* culms, and would gradually increase with further agglutinating of chromatin. Besides, dense $Mg^{2+}$-ATPase was detected in multi-vesicle bodies and disintegrated tonoplast. Generally, $Mg^{2+}$-ATPase in nucleus during plant normal development played important roles in the formation and stabilization of physiological space between nucleosomes, and $Mg^{2+}$-ATPase activity was examined on the nuclear chromatin in cells with active metabolism. Moreover, $Mg^{2+}$-ATPase localized in nuclear chromatin during PCD correlated to the condensation and rupture of chromatin (Tian and Shen, 1996). The dynamic changes of $Mg^{2+}$-ATPase on nuclear chromatin showed that nuclear chromatin of fiber cells actively participated in secondary wall formation. The hydrolization of $Mg^{2+}$-ATPase in nuclear chromatin during fiber PCD could provide energy for accelerating the condensation and rupture of chromatin, which resulted in nDNA degeneration (Andrea *et al.*, 2008). In like manner, $Mg^{2+}$-ATPase localized in disintegrated cytoplasm and multi-vesicle bodies of fiber cells, could be involved in the autolysis of protoplasts, and provided substance for secondary wall formation.

In summary, all evidences including cytology, cytochemistry and TUNEL assay, validated that fiber cell secondary wall formation in *P. edulis* culms was an active PCD. The persistence of plasma membrane and agglutinated nucleus with $Mg^{2+}$-ATPase activity during PCD showed that fiber PCD would keep for a long time until the removal of fiber cell nucleus.

In plants, PCD during normal development has been subdivided into two categories: that is, apoptotic PCD and autophagic PCD involving the early disruption of the vacuole (Bursch, 2001; Bras *et al.*, 2005). Apoptotic PCD in plants is rapid, beginning with the degradation of the nucleus and subsequent incomplete breakdown of cellular organelles, and the cytoplasmic shrinkage and plasmolysis are its typical features. Plant cells during autophagic PCD appeared to be predisposed for quick autolysis, for example, there was an enzymatic apparatus ready to mediate quick specific DNA cleavage triggered by either rapid accidental vacuole disintegration or programmed vacuolar collapse (Hatsugai *et al.*, 2004; Andrea *et al.*, 2008), and the typical cytological changes of autophagic PCD is characterized by the cytoplasmic vacuolation (Bras *et al.*, 2005). Based on the occurrence of plasmolysis and apoptotic bodies, He *et al.* (2000) considered that the PCD of fiber cell in *P. edulis* culms occurred during early secondary wall formation. As in this study, no plasmolysis and apoptotic bodies were detected during fiber development, but the nuclear chromatin agglutination and cytoplasmic vacuolation were examined during the process, which indicated the characteristics of autophagic PCD.

## The role of $Ca^{2+}$ during fiber PCD

In plant cell, calcium may stimulate the calcium-dependent endonuclease and induce DNA decomposition (Xu and Hanson, 2000). Increase in calcium concentration is characteristic of PCD (Qiu *et al.*, 2005). Generally, the increase of $Ca^{2+}$ in cytoplasm can activate a series of $Ca^{2+}$-dependent hydrolase for the disintegration of cytoplasm and nucleus, and then ATP-dependent intake system of $Ca^{2+}$ on karyotheca is also activated resulting in the increase of the level of $Ca^{2+}$ in nucleus. The inflow of $Ca^{2+}$ in cytoplasm contributes to the disintegration of tonoplast and the cease of cytoplasm stream, thereby initiates cell death (Groover and Jones, 1999). According to our investigation, the increase of $Ca^{2+}$ level in cytoplasm coincided with the fiber PCD, which implied that the increased $Ca^{2+}$ in cytoplasm resulted in the disintegration of tonoplast and the release of nuclease, and eventually initiated fiber PCD. During fiber PCD in *P. edulis* culms, the persistence of $Ca^{2+}$ in nucleus could play important roles in chromatin agglutination and DNA degradation.

### The role of APase during fiber PCD

During primary wall formation, APase activity was detected on the nuclear chromatin of fiber cells in *P. edulis* culms, and would increase at the late stage followed by the occurrence of fiber PCD. The developmental process of fiber cell is a continuous process, which included three stages: that is, the formation of fiber initials, primary wall and secondary wall (He *et al.*, 2000; Gan and Ding, 2005). Cui (1997) held that the late stage of primary wall formation may be critical to fiber differentiation and development. Dense APase localized on the chromatin at the critical stage of fiber differentiation indicated that APase was evidently correlated to the occurrence of PCD. During secondary wall formation, APase remained on the agglutinated chromatin, the cytoplasm and tonoplast and mitochondrion of fiber cell, which showed that APase may be involved in the *in situ* autolysis of cytoplasm, and the disintegration of tonoplast and mitochondrion (Wang *et al.*, 1999). Evidently, APase played a crucial role in the disintegration of protoplast during fiber PCD.

**Acknowledgements**: The authors thank technician Xihua Gan, Nanjing Forestry University, for assistance in sample preparation.

### References:

Abd Latif M, 1995. Some selected properties of two Malaysian Bamboo species in relation to age, height, site and seasonal variation [D]. Faculty Forestry, UPM, 281

Andrea K, Zdenek O, Lukas F, 2008. Is internucleosomal DNA fragmentation an indicator of programmed death in plant cells [J]. *Journal of Experimental Botany*, **59** (8): 2233—2240

Bras M, Queenan B, Susin SA, 2005. Programmed cell death via mitochondria: different modes of dying [J]. *Biochemistry (Moscow)*, **70**: 231—239

Bursch W, 2001. The autophagosomal-lysosomal compartment in programmed cell death [J]. *Cell Death and Difference*, **8**: 569—581

Cao J, Jiang F, Sodmergen, Cui KM (崔克明), 2003. Time-course of programmed cell death during leaf senescence in *Eucommia ulmoides* [J]. *Journal of Plant Research*, **116**: 7—12

Cashikar AG, Kumaresan R, Rao NM, 1997. Biochemical characterization and subcellular localization of the red kidney bean purple acid phosphatase [J]. *Plant Physiology*, **114**: 907—915

Cui K M (崔克明), 1997. Switch and stages of plant cell differentiation [J]. *Chinese Life Science* (生命科学), **9**: 49—54

Cui KM (崔克明), 2000. Mechanisms of programmed cell death and its relation to development in plants [J]. *Chinese Bulletin of Botany* (植物学通报), **17** (2): 97—107

Darleen AD, Stillman JI, George SE, 1989. Acid phosphatase localization in seedling tissues of the palms, *Phoenix dactylifera* and *Washingtonia filifera*, and its relevance to controls of germination [J]. *Canadian Journal of Botany*, **67**: 1103—1110

Esauk, 1977. Anatomy of Seed Plants [M]. New York: Wiley, 44—47

Espiloy Z, 1987. Physico-mechanical Properties and Anatomical Relationships of Some Philippine bamboos [A]. In: Rao AN, Dhanarajan G, Sastry CB eds. Recent Research on Bamboo [C].

Ferten N, Moustacas AM, Nari J *et al.*, 2003. Characterization and kinetic properties of a soyabean cell-wall phosphatase [J]. *European Journal of Biochemistry*, **211**: 297—304

Fujii T, 1985. Cell-wall structure of the culm of Azumanezaza (*Pleioblastus chino* Max.) [J]. *Mokuzai Gakhaishi*, **31** (11): 865—872

Fukuda H, 2000. Programmed cell death of tracheary elements as a paradigm in plants [J]. *Plant Molecular Biology*, **44**: 245—253

Gan XH, Ding YL, 2005. Developmental anatomical study on the culm fiber of *Phyllostachys edulis* [J]. *Bamboo Science and Culture*, **19** (1): 16—22

Ghosh SS, Negi BS, 1959. Anatomical features of bamboo used for paper manufacture. Cell. Res. Symp. Council of Scientific and Industrial Research, New Delhi, India. 139—148

Groover A, DeWitt N, Heidel A *et al.*, 1997. Programmed cell death of plant tracheary differentiating *in vitro* [J]. *Protoplasma*, **196**: 197—211

Groover A, Jones AM, 1999. Tracheary element differentiation uses a novel mechanism coodinating progreammed cell death and secondary cell wall synthesis [J]. *Plant Physiology*, **119** (4): 375—384

Gunawardena AHLAN, 2008. Programmed cell death and tissue remodelling in plants [J]. *Journal of Experimental Botany*, **59** (3): 445—451

Gunawardena AHLAN, Greenwood JS, Dengler NG, 2007. Cell wall degradation and modification during programmed cell death in lace plant, *Aponogeton madagascariensis* (Aponogetonaceae) [J]. *American Journal of Botany*, **94**: 1116—1128

Gunawardena AHLAN, Sault K, Donelly P *et al.*, 2005. Programmed cell death and leaf morphogenesis in *Monstera obliqua* (Araceae) [J]. *Planta*, **221**: 607—618

Hatsugai N, Kuroyanagi M, Yamada K *et al.*, 2004. A plant vacuolar protease, VPE, mediates virus-induced hypersensitive cell death [J]. *Science*, **305**: 855—858

He XQ, Wang YQ, Hu YX *et al.*, 2000. Ultrastructural study of secondary wall formation in the stem fibre of *Phyllostachys pubescens* [J]. *Acta Botanica Sinica*, **42**: 1009—1013

Ibrahim H, Pertl H, Pittertschatscher K *et al.*, 2002. Release of an acid phosphatase activity during lily pollen tube growth involves components of the secretory pathway [J]. *Protoplasma*, **219**: 176—183

Jones AM, 2001. Progrommed cell death in development and defense [J]. *Plant Physiology*, **125**: 94—97

Liese W, Grosser D, 1972. Untersuchungen zur Variabilität der Faserlänge bei Bambus [J]. *Holzforsch Holzverwert*, **26** (6): 202—211

Liese W, Weiner G, 1996. Ageing of bamboo culms [J]. *Wood Science and Technology*, **30**: 77—89

McCann MC, Stacey NJ, Roberts K, 2000. Targeted cell death in xylogenesis [A]. In: Bryant JA, Hughes SG, Garland JM, eds. Programmed Cell Death in Animals and Plants [M]. Oxford: BIOS Scientific Publishers Ltd, 193—201

Mittler R, Lam E, 1995. In situ detection of nDNA fragmentation during the differentiation of tracheary elements in higher plants [J]. *Plant Physiology*, **108**: 489—493

Murphy RJ, Alvin KL, 1992. Variation in fibre wall structure of bamboo [J]. *IAWA Bulletin*, **13**: 403—410

Parameswaran N, Liese W, 1976. On the fine structure of bamboo fibres [J]. *Wood Science and Technology*, **10**: 231—246

Parameswaran N, Liese W, 1980. Ultrastructural aspects of bamboo cells [J]. *Cellulose Chemistry Technology*, **14**: 587—609

Qiu YL, Liu RS, Xie CT *et al.*, 2005. The dynamic of calcium pyroantimonate precipitates distribution during megasporegenesis of lettuce (*Lactucasativa* L.) [J]. *Journal of Plant Physiology and Molecular Biology*, **31** (4): 374—382

Shigematsu Y, 1940. On the length and the width of the fibre of kanchiku (*Chimonobambusa marmorea*) [J]. *Jouranl of Japanese Forest Society*, **22**: 693—696

Tian GW (田国伟), Shen JH (申家恒), 1994. The ultracytochemical localization of acid phosphatase activity in wheat during fertilization [J]. *Acta Botanica Sinica* (植物学报), **36**: 251—256

Tian GW (田国伟), Shen JH (申家恒), 1996. Ultracytochemical localization of ATPase on wheat nucellus during degeneration [J]. *Acta Botanica Sinica* (植物学报), **38** (2): 100—104

Tono T, Ono K, 1962. The layered structure and its morphological transformation by acid treatment [J]. *Journal of Japanese Wood Research Society*, **8**: 245—249

van Doorn WG, Woltering EJ, 2005. Many ways to exit? cell death categories in plant [J]. *Trends in Plant Science*, **10**: 117—122

Wang YQ (王雅清), Chai JJ (柴晶晶), Cui KM (崔克明), 1999. Ultracytochemical localization of acid phosphatase during differentiation and dedifferentiation of the secondary xylem in *Eucommia ulmoides* trunk [J]. *Acta Botanica Sinica* (植物学报), **41**: 1155—1159

Wang YQ (王雅清), Kalima NKM, Cui KM (崔克明), 2000. Ultracytochemical localization of ATPase during the secondary xylem differentiation and dedifferentiation in *Eucommia ulmoides* trunk [J]. *Acta Botanica Sinica*, **42** (5): 455—460

White PJ, Broadley MR, 2003. Calcium in plants [J]. *Annuals of Botany*, **92**: 487—511

Xu Y, Hanson MR, 2000. Programmed cell death during pollination-induced petal senescence in *Petunia* [J]. *Plant Physiology*, **122**: 1323—1334

Zhu T, Rost TL, 2000. Directional cell-to-cell communication in the *Arabidopsis* root apical meristem: III. Plasmodesmata turnover and apoptosis in meristem and root cap cells during four weeks after germination [J]. *Protoplasma*, **213**: 99—107